

# The Collective Lamb Shift of a Nanoscale Atomic Vapour Layer within a Sapphire Cavity

T. Peyrot, Y.R.P. Sortais, and A. Browaeys

*Laboratoire Charles Fabry, Institut d'Optique Graduate School,  
CNRS, Université Paris-Saclay, F-91127 Palaiseau Cedex, France*

A. Sargsyan and D. Sarkisyan

*Institute for Physical Research, National Academy of Sciences - Ashtarak 2, 0203, Armenia*

J. Keaveney, I.G. Hughes, and C.S. Adams

*Department of Physics, Rochester Building, Durham University, South Road, Durham DH1 3LE, United Kingdom*

(Dated: April 18, 2018)

We measure the near-resonant transmission of light through a dense medium of potassium vapor confined in a cell with nanometer thickness in order to investigate the origin and validity of the collective Lamb-shift. A complete model including the multiple reflections in the nano-cell accurately reproduces the observed strong asymmetry of the line shape and allows extraction of a density dependent shift of the atomic resonance. We observe an additional, unexpected dependence of this shift with the thickness of the medium. This extra dependence demands further experimental and theoretical investigations.

When many light emitters are subjected to an electromagnetic field with a wavelength  $\lambda$ , they may react collectively to the field [1, 2]. A well-known example of collective response is the enhancement of the decay rate of an atomic ensemble with respect to the individual atom case. Owing to the coupling of atoms via resonant dipole-dipole interactions, it becomes important when the volume of interaction is smaller than  $(\lambda/2\pi)^3$ . Collective effects in light scattering have gained a renewed interest recently with the recognition that they can bias the accuracy of atom-based sensors such as optical clocks by introducing unwanted energy level shifts [3–5]. Alternatively, the collective response can be an asset if properly handled and several recent works suggest how it can be used to enhance light-matter interfaces [6–9].

The resonant dipole-dipole interactions between atoms should lead to a collective frequency shift of the atomic lines [10]. This shift, unfortunately named the cooperative or collective Lamb-shift (CLS) despite its classical nature, depends on the shape of the sample. In the case of an atomic slab of thickness  $L$  and density  $N$  it was predicted to be [10]:

$$\Delta_{\text{CLS}} = \Delta_{\text{LL}} - \frac{3}{4}\Delta_{\text{LL}} \left(1 - \frac{\sin 2kL}{2kL}\right), \quad (1)$$

where  $\Delta_{\text{LL}} = -\pi(N/k^3)\Gamma$  is the Lorentz-Lorenz shift,  $k = 2\pi/\lambda$  is the wave vector and  $\Gamma$  is the natural linewidth of the relevant atomic transition. Four decades later, the first measurements of the CLS were reported using a layer of Fe atoms [11] and a slab of hot alkali vapor [12]. Following these experiments it was pointed out that Eq.(1) is valid only in the low density limit ( $N/k^3 \ll 1$  with  $N$  the density of the vapor [13, 14]), a condition not met by the experiment of [12] for which  $N/k^3 \sim 100$ . Reference [15] suggested that this CLS should only be present when large inhomogeneous broadening is present, such as in hot vapor. However, subsequent experiments on ultracold atoms (insignificant inhomogeneous broadening) either reported a shift consistent with the CLS prediction [16], or a negligible shift [17]. Recently, theoretical

work highlighted that the CLS in a slab geometry [13] should merely arise from cavity interferences between the boundaries of the medium. In contrast to the original suggestion [10], in the cavity viewpoint, the CLS would not be related to the Lorentz local field. Clearly, the situation is confusing and further work is needed to clarify it.

In this letter, we present a new investigation of the origin and validity of the CLS. To do so, we measure the transmission resonance line shape of a dense hot vapor of potassium atoms confined in a slab with nanometer thickness. We develop a new model to interpret the data based on standard mean-field electromagnetism. It includes the multiple reflections due to the cavity formed by the two layers of sapphire enclosing the atomic vapor. We show in particular that Eq. (1) is valid only in the limit of a *low-density* atomic slab surrounded by *vacuum*, neither conditions being fulfilled here. Furthermore, using the model, we deconvolve the cavity effect from the measured transmission and extract the shift of the atomic resonance line as a function of density and thickness. We observe an unexpected oscillatory dependence of the shift with the slab thickness, which indicates that further refinement of the theory is needed in order to fully account for the optical properties of dense media.

We first give a simple derivation of the CLS [Eq.(1)] that highlights the roles of the boundaries and of the dipole-dipole interactions between atoms, as well as its range of applicability. We consider an atomic slab (thickness  $L$ , susceptibility  $\chi$ , refractive index  $n = \sqrt{1 + \chi}$ ) placed in vacuum and illuminated by a plane wave  $E_0 \exp[ikz]$  with frequency  $\omega = ck$ . As the light propagates in the medium, the fields radiated by the induced dipoles interfere with the incident field and in turn excite new atoms: the dipole-dipole interaction, which is the interaction of the field radiated by an atomic dipole with another dipole [18], is thus included in the description of the propagation. The field scattered at position  $z$  by a slice of thickness  $dz' \ll \lambda$  located at position  $z'$  is  $dE_{\text{sc}}(z) = ikP(z')/(2\epsilon_0) \exp[ik|z - z'|]dz'$  [18, 19]. Here

$P(z')$  is the polarization vector related to the *total* field  $E(z')$  inside the medium by  $P(z') = \epsilon_0 \chi E(z')$ . Consequently, the superposition principle yields the field transmitted by the slab:

$$E_t(z > L) = E_0 e^{ikz} + \frac{ik\chi}{2} \int_0^L E(z') e^{ik(z-z')} dz'. \quad (2)$$

To calculate the *total* field inside the slab, we neglect the multiple reflections at the boundaries between the medium and vacuum. Therefore  $E(z') \approx tE_0 e^{inkz'} + rE_0 e^{ink(2L-z')}$ , with  $n \approx 1 + \chi/2$ ,  $t = 2/(n+1) \approx 1 - \chi/4$  and  $r = (n-1)/(n+1) \approx \chi/4$ , for  $\chi \ll 1$ . Using these expressions in Eq. (2) we get, up to second order in  $\chi$ :

$$E_t \approx E_0 e^{ikz} \left[ 1 + i \frac{\chi k L}{2} \left( 1 + i \frac{\chi k L}{4} - \frac{\chi}{4} + \frac{\chi}{4} \frac{e^{2ikL} - 1}{2ikL} \right) \right]. \quad (3)$$

The susceptibility of the dilute slab consisting of atoms with polarizability  $\alpha = i(6\pi\Gamma/k^3)/(\Gamma_t - 2i\Delta)$  ( $\Delta = \omega - \omega_0$  with  $\omega_0$  the resonant frequency,  $\Gamma$  the radiative linewidth and  $\Gamma_t$  the total homogeneous linewidth) is  $\chi = N\alpha$ . Using  $1+x \approx 1/(1-x)$  for  $|x| \ll 1$  in the parenthesis of Eq. (3), we obtain the transmission coefficient:

$$T(\Delta) = \left| \frac{E_t}{E_0} \right|^2 = \left| 1 - \frac{3\pi N L}{k^2} \frac{\Gamma}{\Gamma_c - 2i(\Delta - \Delta_c)} \right|^2, \quad (4)$$

with the thickness dependent shift  $\Delta_c = -\frac{3}{4}\Delta_{LL}(1 - \frac{\sin 2kL}{2kL})$  and  $\Gamma_c = \Gamma_t - \frac{3}{4}(kL + \frac{\sin^2 kL}{kL})\Delta_{LL}$ . The offset  $-\frac{3}{4}\Delta_{LL}$  in the shift is traced back to the transmission through the first interface. To recover the extra offset  $\Delta_{LL}$  in Eq. (1), we must use the Lorentz-Lorenz formula [20] in Eq. (3):  $\chi = N\alpha/(1 - N\alpha/3)$ . This derivation therefore shows that (i) the CLS is a frequency shift of the position of the transmission minimum and not a shift of the resonance  $\omega_0$  of the bulk medium characterized by  $\chi$ ; (ii) it is a consequence of the reflection of the field at the boundaries of the slab; (iii) it includes the dipole-dipole interactions in the propagation and, (iv) Eq. (1) is only valid in a medium for which  $\chi \ll 1$  at resonance, *i.e.*  $(N/k^3)(\Gamma/\Gamma_t) \ll 1$ .

To extend the model beyond the dilute regime we include the multiple reflections in the cavity produced by the interface between the atomic medium and its environment (index  $n_s$ ). Using a textbook interference argument [13], we calculate the transmission coefficient of the field amplitude and get:

$$t(\Delta) = \frac{4n_s n \exp[i(n - n_s)kL]}{(n_s + n)^2 - (n_s - n)^2 \exp[2inkL]}. \quad (5)$$

For  $n_s = 1$ , Eq. (5) predicts that the frequency of the minimum transmission  $\Delta_{\min}$  does follow Eq. (1), but only when  $(N/k^3)(\Gamma/\Gamma_t) \ll 1$  (see Fig. 4 in [14]). This is no longer the case for  $n_s = 1.76$  for which  $\Delta_{\min}$  *never* follows Eq. (1) even at low density (see details in [21]).

We now describe our experimental investigation of the CLS using a nano-cell [22]. The nano-cell (Fig. 1a) consists of two 1 mm-thick sapphire wedge plates ( $n_s = 1.76$ ) filled with a

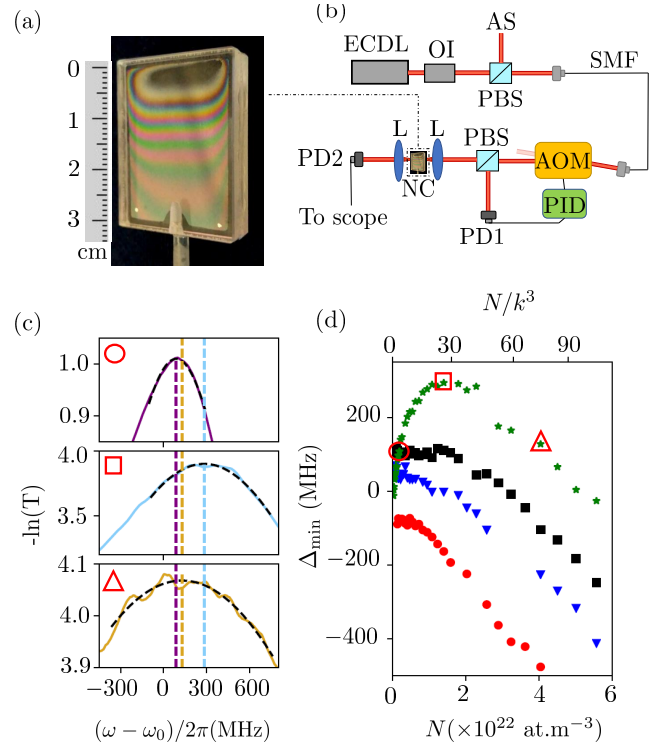


FIG. 1: (a) Nano-cell used in the experiment. The interference fringes indicate that the thickness of the slab between the two sapphire windows varies from 50 nm to 1.5  $\mu\text{m}$  at the bottom. (b) Optical set-up. ECDL: external cavity laser diode; OI: optical isolator; PBS: polarization beam-splitter; SMF: single-mode fiber; NC: nano-cell; PD: photodiode; AOM: acousto-optic modulator; L: lens; AS: absorption spectroscopy; PID: proportional-integral-derivative controller. (c) Measured optical density for a slab of thickness  $L = 490$  nm as a function of the detuning and for temperatures  $\Theta = (260^\circ\text{C}, 340^\circ\text{C}, 380^\circ\text{C})$  (top, middle, bottom), corresponding to  $N/k^3 = (3, 29, 74)$ . Vertical dotted lines: frequency  $\Delta_{\min}$  of the maximum of the OD. (d)  $\Delta_{\min}$  versus density  $N$  for  $L = 90$  nm (red dots),  $L = 110$  nm (blue triangles),  $L = \lambda/2 = 380$  nm (black squares) and  $L = 3\lambda/4 = 575$  nm (green stars). The empty square, triangle and circle correspond to the curves in (c).

vapor of potassium [23]. The resulting atomic slab has a thickness  $L$  varying between 50 nm and 1.5  $\mu\text{m}$  [24]. The atomic density is controlled by heating the cell from room temperature up to 380°C, achieving similar densities as in [12]. Compared to the earlier measurements performed in rubidium [12], potassium has the advantage of a smaller hyperfine splitting in the ground state, which results into a single atomic line at lower densities. The optical set-up is shown in Fig. 1(b). We measure the transmission of a laser beam nearly resonant with the D2 transition of  $^{39}\text{K}$  ( $\lambda \approx 767$  nm,  $\Gamma = 2\pi \times 6$  MHz). The beam is produced by a commercial external cavity laser diode, focused on the cell sapphire windows with a waist  $w \approx 40$   $\mu\text{m}$   $\gg L$ . We use the interferometric techniques described in [25] to measure the local thickness. The laser is scanned across the resonance over a range of about 30 GHz. The intensity is stabilized using a PID-controlled acousto-optic modulator [26].

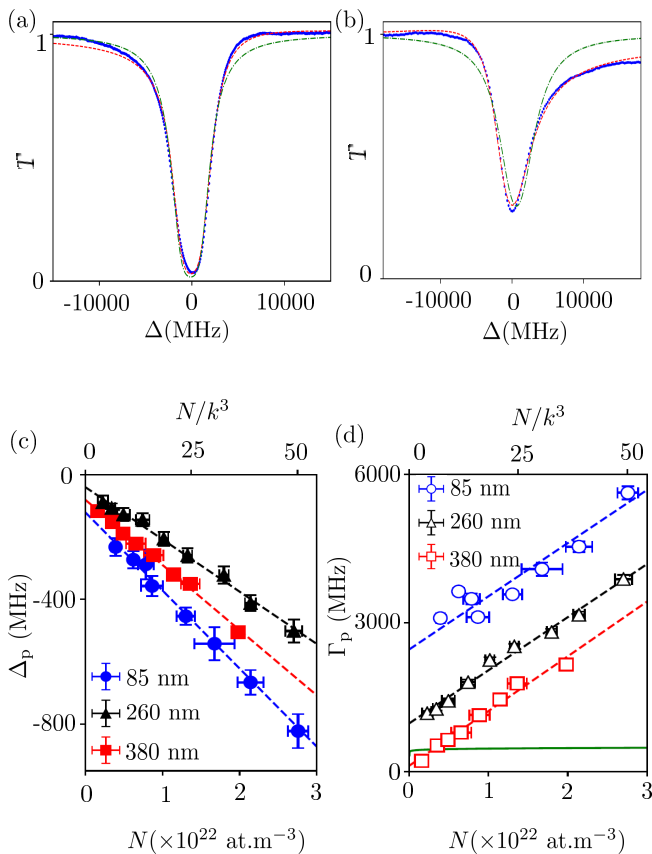


FIG. 2: Top panels represent transmission profiles for (a)  $\Theta = 330^\circ\text{C}$  and  $L = 440\text{ nm}$  and (b)  $\Theta = 365^\circ\text{C}$  at  $L = \lambda/4$  where the asymmetry is most pronounced. Blue dots: measured transmission. Green line: transmission calculated with the model where  $n_s = 1$ . Red dashed line: transmission calculated by the cavity model where  $n_s = 1.76$ . (c) Experimental shift  $\Delta_p$  and (d) broadening  $\Gamma_p$  for various cell thicknesses  $L$ . Solid line: Doppler width. The dashed lines are linear fits to the data. The error bars on both axes are extracted from the fit.

The frequency of the laser is calibrated by standard saturated absorption spectroscopy in a 7.5 cm potassium reference cell.

Figure 1(c) shows the measured optical density OD, extracted from the transmission  $T$  via  $\text{OD} = -\ln(T)$ , as a function of the laser detuning  $\Delta$  for three values of the atomic density  $N$ . We plot  $\Delta_{\min}$ , defined as the detuning at which the OD is the largest, as a function of density for various thicknesses  $L$  in Fig. 1(d). At high density ( $N/k^3 \gtrsim 20$ ) we observe a red-shifted, linear variation of  $\Delta_{\min}$  with  $N$  for all  $L$ . At low  $N$ , for  $L > \lambda/2$ ,  $\Delta_{\min}$  exhibits a pronounced blue-shift, and turns into a red-shift at higher density. For thicknesses  $L \lesssim \lambda/2$ ,  $\Delta_{\min}$  features a plateau at low  $N$ , as also seen in [12]. Similar blue-shifts of the minimal transmission were observed in a nano-cell of cesium [27], although much smaller than here, and recently in a slab of ultra-cold rubidium atoms [17], where an evolution from the blue to the red side of the resonance was also measured.

To explain the data, we now develop a model that decon-

volves the effect of the cavity produced by the interface between the sapphire windows and the atomic medium, and the bulk properties of the atomic medium. This was also the approach used in Ref. [12]. However, the model used there to extract the shift took only partially the cavity effect into account (see details in [21]). Furthermore, as explained above Eq. (1) is irrelevant for the experimental situation of a nano-cell: the atomic slab should be dilute and surrounded by vacuum for the formula to hold. The agreement between the measured shift as a function of the cell thickness and Eq. (1) must therefore be considered as fortuitous.

Our new model incorporates the multiple reflections in the cavity by using Eq. (5). As for the atomic slab, it is described by a continuous resonant medium with a refractive index  $n$ . Ascribing a refractive index to a hot vapor confined in a nano-cell is far from being obvious, as has been studied in great details (e.g. [28–31]). First, the Doppler effect leads to a non-local refractive index, and second, the small thickness of the cell results in a non-steady state response of most atoms but the ones flying parallel to the cell surface. However, when the density is as large as the ones used here, the collisional broadening of the line  $\Gamma_p$  exceeds the Doppler width  $\Delta\omega_D$  (see below and Fig. 2d): the atomic dipoles reach their steady-state over a distance  $\sim \Delta\omega_D/(k\Gamma_p)$ , much smaller than  $L$  and  $\lambda$ . It then becomes possible to define a *steady-state, local* refractive index [29].

We relate the refractive index of the atomic slab to the electric susceptibility  $\chi$  by  $n(\Delta) = \sqrt{1 + \chi(\Delta)}$ . Here we take  $\chi = N\alpha_p$  with  $\alpha_p(\Delta, N)$  the polarizability of the atoms, including the influence of the density at the single atom level through a broadening and a shift. It is calculated by summing the contribution of all hyperfine transitions of the D2 line with Lorentzian profiles, weighted by the corresponding Clebsch-Gordan coefficients [32] ( $\Gamma$  is the radiative decay rate of the strongest transition):

$$\alpha_p(\Delta, N) = i \frac{6\pi\Gamma}{k^3} \sum_{F, F'} \frac{C_{FF'}^2}{\Gamma_t - 2i\Delta_t}. \quad (6)$$

Here, we do not integrate over the velocity distribution, as Doppler broadening is negligible with respect to the homogeneous broadening [33]. In Eq. (6),  $\Gamma_t = \Gamma + \Gamma_p$  is the sum of the radiative linewidth  $\Gamma$  and a width  $\Gamma_p$  that accounts in a phenomenological way for any broadening mechanism inside the gas beyond the cavity-induced broadening. In the same way, the detuning  $\Delta_t = \Delta + \Delta_{FF'} + \Delta_p$ , with  $\Delta_{FF'}$  the hyperfine splitting and  $\Delta_p$  a phenomenological shift inside the gas beyond the cavity-induced shift. The quantities  $\Delta_p(N, L)$  and  $\Gamma_p(N, L)$  therefore contain the physics not included in the model: (i) the interaction of the atoms with the cell walls (only dependent on the thickness  $L$ ), (ii) the collisional dipole-dipole interactions between the light-induced dipoles (only dependent on the density  $N$ ), and (iii) any extra effects that may depend both on  $L$  and  $N$ . Finally, to compare our model to the data, we normalize the transmission coefficient in intensity to the non-resonant case ( $n = 1$ ):

$$T = |t(\Delta)/t(\Delta \rightarrow \infty)|^2.$$

Figures 2(a-b) show a comparison of the model's prediction and the measured line shape. The agreement is very good. In particular, the model reproduces the observed asymmetric line shape, and the blue shift of the maximum optical depth observed in Fig. 1(d) (see more details in [21]). To demonstrate the importance of the sapphire layers in the optical response, we also plot in Fig. 2(a) the result of Eq. (5) for the case of an atomic layer immersed in vacuum ( $n_s = 1$ ): there the asymmetry is nearly absent.

To fit the data by the model and obtain the good agreement shown in Figs. 2(a,b), we let the density  $N$  (or equivalently the temperature  $\Theta$  [34]), the line shift  $\Delta_p$  and the broadening  $\Gamma_p$  as free parameters. In Figs. 2(c,d) we plot the fitted values of  $\Delta_p$  and  $\Gamma_p$  as a function of the fitted  $N$ , for various thicknesses. Both  $\Delta_p$  and  $\Gamma_p$  have an offset at asymptotically low density, that increases when the thickness of the cell decreases. Its origin lies in the interaction between the atoms and the walls of the nano-cell, as was measured in Ref. [35]: when the thickness decreases, the fraction of atoms interacting significantly with the cell walls increases. Figure 2(d) indicates that  $\Gamma_p$  is much larger than the Doppler width and the broadening is dominated by the density-dependent contribution coming from the collisional dipole-dipole interactions. For the range of densities explored here, the vapor is thus homogeneously broadened with  $(N/k^3)(\Gamma/\Gamma_t) \lesssim 1$ .

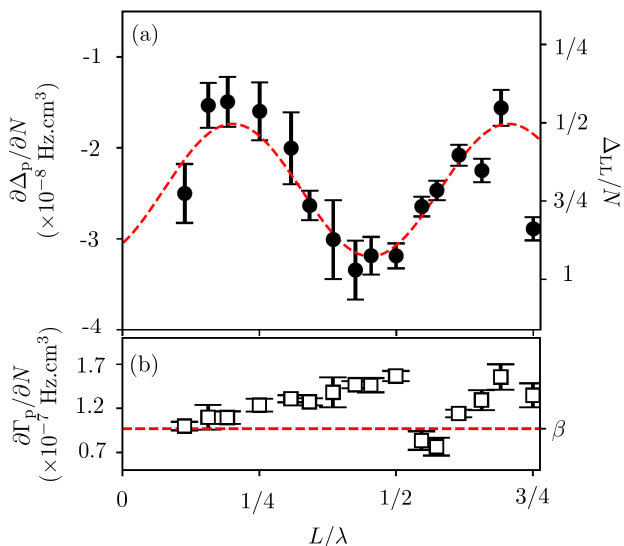


FIG. 3: (a) Black dots: slope  $\partial\Delta_p/\partial N$  of the shift extracted from the cavity model as a function of the cell thickness  $L$ , together with the fit by a sinusoidal function (dashed red line). (b) Black empty squares: slope  $\partial\Gamma_p/\partial N$  of the width extracted from the cavity model as a function  $L$ . The red dashed line is the theoretical value of the self-broadening coefficient  $\beta$  resulting from the collisional interactions between atoms (see text). The errors bars are dominated by the systematic effects detailed in [21].

To remove the influence of the surface on the shift (an effect depending on  $L$  only), we fit the data presented in Figs. 2(c,d)

by a linear function and extract the slopes  $(\partial\Delta_p/\partial N)(L)$  and  $(\partial\Gamma_p/\partial N)(L)$ . We plot in Figs. 3(a,b) these slopes as a function of the thickness  $L$ . Both quantities feature an offset that we attribute to collisional dipole-dipole interactions between atoms. For example, the offset on  $\partial\Gamma_p/\partial N$  extracted from Fig. 2(d) is close to the calculated self-broadening coefficient resulting from the collisional dipole-dipole interactions  $\beta = 2\pi\sqrt{2}\Gamma/k^3$  [36] (dotted line in Fig. 3b). However we also observe a residual oscillation of the shift slope with a period  $(0.5 \pm 0.02)\lambda$  (the error bars are discussed in [21]). This oscillation is unexpected: all known dependences of  $\Delta_p$  with the cell thickness is included and should result in a shift slope being a bulk property of the medium, independent of  $L$ .

We finally examine possible explanations for the residual shift shown in Fig. 3(a). A first possibility could be a non-Maxwellian velocity distribution due to the cell surface [37]. Dicke coherent narrowing [38], which depends on the cell thickness is also expected in nano-cells. However the measured line width  $\Gamma_p$  is much larger than the expected Doppler width and any modifications of the velocity distribution should have a negligible effect on the extracted value of  $\Delta_p$ . A second possibility could be the influence of the correlations among dipoles induced by the interactions. They are ignored in our treatment of the configuration-averaged field and in all the models developed so far [10, 13–15, 39, 40]. This assumption is valid for dilute gases but it could fail at higher densities such as the ones explored here. Going beyond a mean-field approach by including them could lead to a non-local response of the gas. The models presented here or in Refs. [10, 13–15], which assume a local susceptibility, would then fail – and including the correlations would be a highly non-trivial undertaking.

In conclusion, we have performed a new series of measurements of the transmission of near-resonant light through an alkali vapor with nanometer scale thickness in order to investigate the origin and validity of the collective Lamb-shift. A model, deconvolving the cavity effect from the atomic properties of the slab, accurately reproduces the observed strong asymmetry of the line shape. Using this model we extract from our data a shift of the bulk atomic medium resonance, which oscillates with the thickness of the medium. The origin of this oscillation is not understood and we have formulated a few directions that should be explored theoretically.

We acknowledge fruitful discussions with J. Ruostekoski. T. Peyrot is supported by the DGA-DSTL fellowship 2015600028. We also acknowledge financial support from EPSRC (grant EP/L023024/1) and Durham University. The data presented in this paper will be available later on.

- 
- [1] M. Gross and S. Haroche, Superradiance: an essay on the theory of collective spontaneous emission, *Phys. Rep.* **93**, 301 (1982).
  - [2] W. Guérin, M.T. Rouabah and R. Kaiser, Light interacting with atomic ensembles: collective, cooperative and mesoscopic ef-



- fects, *J. Mod. Optics* **64**, 895 (2017).
- [3] D.E. Chang, J. Ye and M.D. Lukin, Controlling dipole-dipole frequency shifts in a lattice-based optical atomic clock, *Phys. Rev. A* **69**, 023810 (2004)
- [4] S.L. Bromley *et al.*, Collective atomic scattering and motional effects in a dense coherent medium, *Nat. Comm.* **7**, 11039 (2016).
- [5] S.L. Campbell *et al.*, A Fermi-degenerate three-dimensional optical lattice clock, *Science*. **358**, 6359 (2017)
- [6] R.J. Bettles, S.A. Gardiner and C.S. Adams, Cooperative ordering in lattices of interacting two-level dipoles, *Phys. Rev. A* **92**, 063822 (2015).
- [7] R.J. Bettles, S.A. Gardiner and C.S. Adams, Enhanced optical cross section via collective coupling of atomic dipoles in a 2D array, *Phys. Rev. Lett.* **116**, 103602 (2016).
- [8] E. Shahmoon, D.S. Wild, M.D. Lukin and S.F. Yelin, Cooperative resonances in light scattering from two-dimensional atomic arrays, *Phys. Rev. Lett.* **118**, 113601 (2017)
- [9] J. Perczel *et al.*, Topological quantum optics in two-dimensional atomic arrays, *Phys. Rev. Lett.* **119**, 023603 (2017)
- [10] R. Friedberg, S.R. Hartmann and J.T. Manassah, Frequency shift and absorption by resonant systems of two-level atoms, *Phys. Rep.* **7**, 101 (1973).
- [11] R. Röhlsberger, K. Schlage, B. Sahoo, S. Couet and R. Roeffler, Collective Lamb shift in single-photon superradiance, *Science* **328**, 1248 (2010).
- [12] J. Keaveney, A. Sargsyan, U. Krohn, I.G. Hughes, D. Sarkisyan and C.S. Adams, Cooperative Lamb shift in an atomic vapor layer of nanometer thickness, *Phys. Rev. Lett.* **108**, 173601 (2012).
- [13] J. Javanainen and J. Ruostekoski, Light propagation beyond the mean-field theory of standard optics, *Optics Express*, **24**, 993 (2016).
- [14] J. Javanainen, J. Ruostekoski, Y. Li and S.-M. Yoo, Exact electrodynamics versus standard optics for a slab of cold dense gas, *Phys. Rev. A* **96**, 033835 (2017)
- [15] J. Javanainen, J. Ruostekoski, Y. Li and S.-M. Yoo, Shifts of a resonance line in a dense atomic sample, *Phys. Rev. Lett.* **112**, 113603 (2014).
- [16] S.J. Roof, K.J. Kemp, M.D. Havey and I.M. Sokolov, Observation of single-photon superradiance and the cooperative Lamb shift in an extended sample of cold atoms, *Phys. Rev. Lett.* **117**, 073003 (2016).
- [17] L. Corman, J.-L. Ville, R. Saint-Jalm, M. Aidelsburger, T. Bienaimé, S. Nascimbène, J. Dalibard and J. Beugnon, Transmission of near-resonant light through a dense slab of cold atoms, *Phys. Rev. A* **96**, 053629 (2017).
- [18] H. Fearn, D.F.V. James, and P. Milonni, Microscopic approach to reflection, transmission and the Ewald-Osen extinction theorem, *Am. J. Phys.* **64**, 986 (1996).
- [19] R.P. Feynman, R.B. Leighton, and M. Sands, *Lectures on Physics*, vol. 1, chap. 30, Addison Wesley (2006).
- [20] J.D. Jackson, *Classical Electrodynamics*, (John Wiley and Sons, New York, 1998).
- [21] See Supplemental Material.
- [22] D. Sarkisyan, T. Varzhapetyan, A. Sarkisyan, Y. Malakyan, A. Papoyan, A. Lezama, D. Bloch and M. Ducloy, Spectroscopy in an extremely thin vapor cell: Comparing the cell-length dependence in fluorescence and in absorption techniques, *Phys. Rev. A* **69**, 065802 (2004).
- [23] To avoid cavity effect from the sapphire plates, they form a wedge with an angle of 10 mrad, much larger than the 0.1 mrad angle of the atomic slab.
- [24] A. Sargsyan, A. Tonoyan, *et al.*, Complete hyperfine Paschen-Back regime at relatively small magnetic fields realized in potassium nano-cell. *Europhysics Letters* **110**, 23001 (2015).
- [25] E. Jahier, J. Guéna, P. Jacquier, M. Lintz, A.V. Papoyan and M.A. Bouchiat, Temperature-tunable sapphire windows for reflection loss-free operation of vapor cells, *Appl. Phys. B* **71**, 561 (2000).
- [26] G. Truong, J.D. Anstie, E.F. May, T.M. Stace and A.N. Luiten, Absolute absorption line-shape measurements at the shot-noise limit, *Phys. Rev. A* **86**, 030501 (2012)
- [27] I. Maurin, P. Todorov, I. Hamdi, A. Yarovitski, G. Dutier, D. Sarkisyan, S. Saltiel, M.-P. Gorza, M. Fichet, D. Bloch and M. Ducloy, Probing an atomic gas confined in a nanocell, *J. Physics: Conference Series* **19**, 20 (2005).
- [28] M.F.H. Schuurmans, Spectral narrowing of selective reflection, *J. Phys. France* **37**, 469 (1976).
- [29] T.A. Vartanyan and D.L. Lin, Enhanced selective reflection from a thin layer of a dilute gaseous medium, *Phys. Rev. A* **51**, 1959 (1995).
- [30] B. Zambon and G. Nienhuis, Reflection and transmission of light by thin vapor layers, *Opt. Comm.* **143**, 308 (1997).
- [31] G. Dutier, S. Saltiel, D. Bloch, and M. Ducloy, Revisiting optical spectroscopy in a thin vapor cell: mixing of reflection and transmission as a Fabry-Perot microcavity effect, *JOSA B* **20**, 793 (2003).
- [32] M.A. Zentile, J. Keaveney, L. Weller, D.J. Whiting, C.S. Adams and I.G. Hughes, ElecSus: A program to calculate the electric susceptibility of an atomic ensemble, *Comp. Phys. Comm.* **189**, 162 (2015).
- [33] By performing the integration over the velocity distribution, we have checked that it indeed has no effect.
- [34] Although the temperature is left as a free parameter here, the fitted values are very close to the values measured on the experiment by the thermocouple in contact with the reservoir.
- [35] K.A. Whittaker, J. Keaveney, I.G. Hughes, A. Sargsyan, D. Sarkisyan and C.S. Adams, Optical response of gas-phase atoms at less than  $\lambda/80$  from a dielectric surface, *Phys. Rev. Lett.* **112**, 253201 (2014).
- [36] L. Weller, R.J. Bettles, P. Siddons, C.S. Adams and I.G. Hughes, Absolute absorption on the rubidium D1 line including resonant dipole-dipole interactions, *J. Phys. B* **44**, 195006 (2011).
- [37] P. Todorov, D. Bloch, Testing the limits of the Maxwell distribution of velocities for atoms flying nearly parallel to the walls of a thin cell, *The Journal of Chemical Physics* **147**, 194202 (2017).
- [38] G. Dutier, A. Yarovitski, S. Saltiel, A. Papoyan, D. Sarkisyan, D. Bloch and M. Ducloy, Collapse and revival of a Dicke-type coherent narrowing in a sub-micron thick vapor cell transmission spectroscopy, *Europhysics Letters* **63**, 35 (2003).
- [39] O. Morice, Y. Castin and J. Dalibard, Refractive index of a dilute Bose gas, *Phys. Rev. A* **51**, 3896 (1995).
- [40] J. Ruostekoski and J. Javanainen, Quantum field theory of cooperative atom response: Low light intensity, *Phys. Rev. A* **55**, 513 (1997).

## Supplemental Material: The Collective Lamb Shift of a Nanoscale Atomic Vapour Layer within a Sapphire Cavity

T. Peyrot, Y.R.P. Sortais, and A. Browaeys

*Laboratoire Charles Fabry, Institut d'Optique Graduate School,  
CNRS, Université Paris-Saclay, F-91127 Palaiseau Cedex, France*

A. Sargsyan and D. Sarkisyan

*2 Institute for Physical Research, National Academy of Sciences - Ashtarak 2, 0203, Armenia*

J. Keaveney, I.G. Hughes, and C.S. Adams

*Department of Physics, Rochester Building, Durham University,  
South Road, Durham DH1 3LE, United Kingdom*

(Dated: April 18, 2018)

In this Supplemental Material, we first provide more informations about the model used in Ref. [1] to extract the Collective Lamb Shift in a nanocell of rubidium. We then show that the cavity model introduced in the main text reproduces the transition from the blue to the red side of the atomic resonance. In the third section, we compare the situation of an atomic slab placed in vacuum to the case where it is placed between two sapphire plates. In the last section, we explain how the error bars displayed in Figs. 3(a,b) of the main text are calculated.

### I. MODEL USED IN REF. [1] TO EXTRACT THE CLS SHIFT

The model developed in [1] relies on two ingredients. First, a model to calculate the susceptibility  $\chi$  of the atomic slab, and therefore its refractive index. This model is the same as the one we used in the present work, with the same free parameters  $\Delta_p$  and  $\Gamma_p$  and density  $N$ . Second, a model to include the cavity surrounding the slab, which we now describe.

The cavity model used the following formula for the transmission of the atomic slab (refractive index  $n$ ) contained between the two sapphire plates (refractive index  $n_s$ ):

$$T_r(\Delta) = T(\Delta) \frac{1 - R[n(\Delta)]}{1 - R[n = 1]} . \quad (1)$$

Here,  $T(\Delta)$  was assumed to follow a Beer-Lambert attenuation:  $T(\Delta) = e^{-2n''(\Delta)kL}$  where  $k = 2\pi/\lambda$  is the wave vector of light in vacuum,  $L$  is the cell thickness and  $n'' = \text{Im}[\sqrt{1 + \chi}]$  with  $\chi$  the susceptibility of the atomic vapor. The susceptibility was calculated using the multilevel model described in the main text.

The reflection coefficient in intensity  $R[n(\Delta)]$  was calculated using the formalism developed in Ref. [2]:

$$R[n(\Delta)] = \left| \frac{Z_{\text{in}} - Z_s}{Z_{\text{in}} + Z_s} \right|^2, \quad (2)$$

with

$$Z_{\text{in}} = \frac{Z_s - iZ_n \tan(kL)}{1 - i(Z_s/Z_n) \tan(kL)}. \quad (3)$$

In this last equation,  $Z_n = 1/n(\Delta)$ , with  $n = \sqrt{1 + \chi}$ , and  $Z_s = 1/n_s$ . The factor  $1 - R[n(\Delta)]$  was phenomenologically introduced to account for the light reflected by the cavity formed by the two sapphire plates. When using Eq.(2), Ref. [1] assumed that the refractive index of the atomic slab was equal to 1. Although this approximation is very good for dilute system, it is not valid close to the resonance for the densities reached in the experiment, where  $\text{Re}[n]$  can be as high as 1.3 [3]. Consequently the approximation made in [1] did not include the cavity effects in an accurate way.

Using this cavity model, Ref. [1], fitted the data to extract  $\Delta_p$  and  $\Gamma_p$ , as we did in the present work. The authors plotted the gradient  $\partial\Delta_p/\partial N$  as a function of the cell thickness  $L$  and found that it agreed with the CLS formula [Eq. (1) of main text]. However, considering the facts that (i) the cavity effect being independently taken into account,  $\Delta_p$  cannot be compared to the CLS, which only originates from the cavity, (ii) the cavity model used to extract  $\Delta_p$  was not accurately taken into account, and (iii) the CLS formula *does not* apply to an atomic slab placed between two sapphire plates (see also Sec. III), the agreement between the shift measured in [3] and the CLS formula must be considered fortuitous. We note here that if we apply the model described in this section (used in Ref. [1]) to our new potassium data, we find the same dependence of the shift slope  $\partial\Delta_p/\partial N$  with  $L$  as the one obtained in Ref. [1] using rubidium. This indicates that our new measurements are compatible with the ones on rubidium.

## II. TRANSITION FROM BLUE TO RED SHIFT IN THE CAVITY MODEL

In this second Section we show that the cavity model introduced in the main text reproduces the transition of the frequency  $\Delta_{\text{min}}$  of the largest optical depth from the blue to the red side of the resonance.

For each measured transmission spectra, we fit the data by the cavity model and extract the three parameters  $(N, \Gamma_p, \Delta_p)$ . We then calculate from these best theoretical spectra the frequency detunings  $\Delta_{\text{min}}$  corresponding to the largest optical depths. Examples of results are plotted in Fig. 1 for a cell thickness  $L = 490$  nm, together with the measured values. We observe that the transition from blue to red with increasing density is qualitatively reproduced by the cavity model. However, there is no quantitative agreement despite the fact the cavity model does reproduce well the measured line shape. The discrepancy

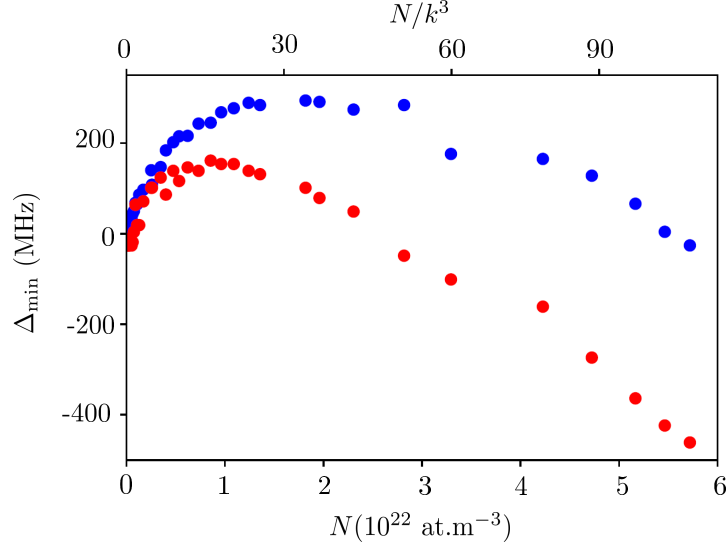


FIG. 1: Value of  $\Delta_{\min}$  for  $L = 490$  nm as a function of  $N$ . Blue dots: experimental values. Red dots: value from the best theoretical fit by the cavity model.

between measured and calculated values of  $\Delta_{\min}$  is nonetheless smaller than a tenth of the linewidth of the line, making it sensitive to possible systematic errors, such as the normalization procedure that we detail in Section IV. However, as we show in Section IV, the oscillations observed in  $\Delta_p$  in Fig. 3(a) are robust against these systematics.

Finally, one way to understand qualitatively the asymmetry of the line and the blue shift observed at low densities uses the complex susceptibility  $\chi$  of the vapor. It has a Lorentzian profile and is proportional to  $N$ . When  $N$  increases the imaginary part  $n''$  of the index of refraction  $n = \sqrt{1 + \chi}$ , is a combination of the real and imaginary parts of  $\chi$ . This is enough to lead to an asymmetry of the line and a blue shift of  $n''$ , and hence of the transmission line.

### III. COMPARISON OF AN ATOMIC SLAB IN VACUUM AND BETWEEN TWO SAPPHIRE PLATES

In this third section, we compare the situation of an atomic slab placed in vacuum or between two plates of refractive index  $n_s$ , as is the case for a nano-cell. We model the atomic vapor by a continuous medium with a susceptibility given by  $\chi = N\alpha$ , where  $\alpha = i(6\pi\Gamma/k^3)/(\Gamma_t - 2i\Delta)$  is the polarizability of the atoms, and a refractive index  $n = \sqrt{1 + \chi}$ .

We use Eq. (5) of the main text for the transmission coefficient. We calculate the frequency  $\Delta_{\min}^{\text{theo}}/|\Delta_{\text{LL}}|$  corresponding to the minimum of transmission for different values of the density and cell thickness. We plot in Fig. 2 the results for two densities corresponding to  $(N/k^3)(\Gamma/\Gamma_t) = 0.01$  and 0.2, for the case of



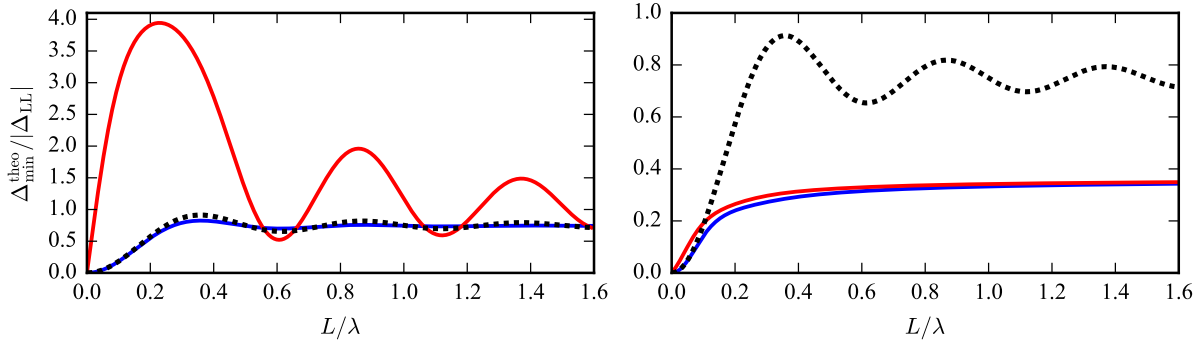


FIG. 2: Frequency  $\Delta_{\min}^{\text{theo}}/|\Delta_{\text{LL}}|$  of the minimum of transmission as a function of the cell thickness for two values of the density corresponding to  $(N/k^3)(\Gamma/\Gamma_t) = 0.008$  (left) and 0.2 (right). The black dashed line is the prediction of the thickness dependent part of the CLS [Eq.(1) of main text]. The solid lines correspond to the predictions of the cavity model developed in the main text for a slab in vacuum ( $n_s = 1$ , blue solid line) or between two sapphire plates ( $n_s = 1.76$ , red solid line).

a slab immersed in vacuum ( $n_s = 1$ ) or placed between two sapphire plates ( $n_s = 1.76$ ). We also plot the prediction of the thickness dependent CLS for  $\chi = N\alpha$  (see main text):  $\Delta_c = -\frac{3}{4}\Delta_{\text{LL}}\left(1 - \frac{\sin 2kL}{2kL}\right)$ . Note that taking for the susceptibility the Lorentz-Lorenz expression  $\chi = N\alpha/(1 - N\alpha/3)$ , would simply offset all predictions of  $\Delta_{\min}^{\text{theo}}/|\Delta_{\text{LL}}|$  in fig. 2 by  $-1$ ; in particular we would recover the prediction of Eq.(1) of the main text for the CLS.

We observe that at low density and for a slab immersed in vacuum, the frequency of the minimum of transmission follows the prediction of the CLS formula (the agreement is perfect at asymptotically low density). However, when the slab is confined between sapphire plates, this is no longer the case: there the multiple reflections induced by the cavity cannot be neglected, as is the case to derive the CLS formula (see main text). At higher density, the frequency of the minimum of transmission deviates from the prediction of the CLS formula. The frequency  $\Delta_{\min}^{\text{theo}}$  becomes independent of the thickness of the cell when the density increases and is nearly identical for the case of vacuum and sapphire.

Experimentally, however, it is not possible to check directly this prediction by studying the frequency of the transmission minimum  $\Delta_{\min}^{\text{exp}}$ :  $\Delta_{\min}^{\text{exp}}$  also depends on the cell thickness via the surface interaction (offset of  $\Delta_p$  in Fig.2c of main text), adding an extra dependence with  $L$ .

#### IV. DISCUSSION OF SYSTEMATIC ERRORS AND CALCULATION OF THE ERROR BARS ON $\partial\Delta_p/\partial N$ AND $\partial\Gamma_p/\partial N$

In this last Section we explain how we calculate the error bars on the slopes  $\partial\Delta_p/\partial N$  and  $\partial\Gamma_p/\partial N$  shown in Figs. 3(a,b) of the main text. We show in particular that the oscillations observed in Fig. 3(a) are robust against possible systematic effects. This discussion is necessary for two reasons. Firstly, as we saw in Sec. II, despite the fact that the cavity model reproduces very well the lineshape of the transmission signal, it fails to yield the measured value of  $\Delta_{\min}$ . The difference between the measured values and the values extracted from the cavity model is on the same order than the values of the shift of interest  $\Delta_p$  obtained by a fit of the line shape with a very small error bar. This indicates that the error bars from the fit possibly underestimate systematic effects. Secondly, as pointed out in the main text, we stabilized the intensity of the laser during the scan. However a small residual variation is possible, that would lead to an enhancement or a reduction of the asymmetry of the line, thus translating into a possible bias on the fitted value of  $\Delta_p$ .

To test the influence of a residual variation of intensity during the scan on the result of the fit yielding  $\Delta_p$  and  $\Gamma_p$ , we study two different ways of normalizing the data: (1) normalization by a linear function interpolating the first and last points of the spectrum, (2) normalization by the first value of the transmission of the spectrum, which therefore yields  $T = 1$ . We fit the lines, normalized by the two procedures, by the cavity model and extract  $\Delta_p$  and  $\Gamma_p$ , together with their error bars. We finally extract the slopes  $\partial\Delta_p/\partial N$  and  $\partial\Gamma_p/\partial N$ , together with the error bars from the fit.

Figure 3 shows the results for the slopes as a function of the cell thickness  $L$  for both procedures. We observe that the variations are similar, but that the results arising from the two normalizations differ by more than the error bars from the fit. Consequently, we calculate the error bars corresponding to the systematic effects from the normalization as being the half difference between the results for the two procedures, for a given thickness. In the main text we show the results corresponding to the second normalization procedure that does not depend on any normalization slope. The final error bars displayed in Figs. 3(a,b) of the main text are the quadratic sum of the systematic and statistical errors (extracted from a set of 5 measurements) as well as of the errors from the fit.

- 
- [1] J. Keaveney, A. Sargsyan, U. Krohn, I.G. Hughes, D. Sarkisyan and C.S. Adams, Cooperative Lamb shift in an atomic vapor layer of nanometer thickness, *Phys. Rev. Lett.* **108**, 173601 (2012).
  - [2] G Brooker, *Modern Classical optics*, OUP, Oxford (2002).
  - [3] J. Keaveney, I.G. Hughes, A. Sargsyan, D. Sarkisyan, and C.S. Adams, Maximal refraction and superluminal

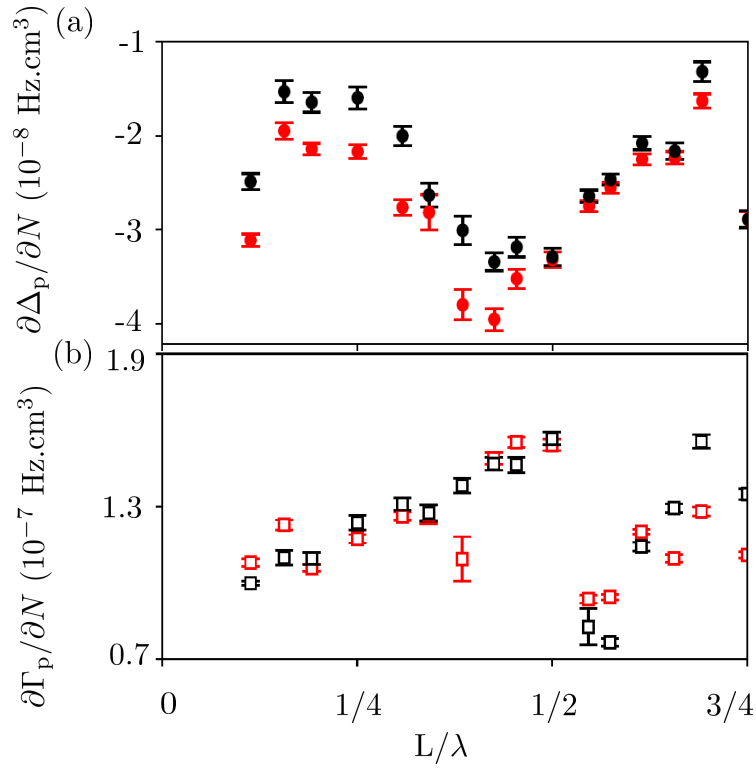


FIG. 3: (a) Slope of the shift  $(\partial\Delta_p/\partial N)(L)$  extracted from the cavity model as a function of the cell thickness  $L$ . (b) Slope of the width  $(\partial\Gamma_p/\partial N)(L)$  from the cavity model. (All figures) Red markers: normalization procedure (1), see text. Black markers: normalization procedure (2). Here, the error bars are given by the fit.

propagation in a gaseous nanolayer, [Phys. Rev. Lett. \*\*109\*\*, 233001 \(2012\)](#).

- [4] R. Friedberg, S.R. Hartmann and J.T. Manassah, Frequency shift and absorption by resonant systems of two-level atoms, [Phys. Rep. \*\*7\*\*, 101 \(1973\)](#).